

Generation of intermediate-depth earthquakes by self-localizing thermal runaway

Timm John^{1*}†, Sergei Medvedev¹, Lars H. Rüpke^{1,2}, Torgeir B. Andersen¹, Yuri Y. Podladchikov¹ and Håkon Austrheim¹

Intermediate-depth (50–300 km) earthquakes commonly occur along convergent plate margins but their causes remain unclear. In the absence of pore-fluid pressures that are sufficiently high to counter the confining pressure in such settings, brittle failure is unlikely. In such conditions, the rocks could fail by the mechanism of progressively self-localizing thermal runaway¹, whereby ductile deformation in shear zones leads to heating, thermal softening and weakening of rock^{1–3}. Here we test this hypothesis by focusing on fault veins of glassy rock (pseudotachylyte) formed by fast melting during a seismic event, as well as associated ductile shear zones that occur in a Precambrian terrane in Norway. Our field observations suggest that the pseudotachylytes as well as shear zones have a single-event deformation history, and we also document mineralogical evidence for interaction of the rocks with external fluids. Using fully coupled thermal and viscoelastic models, we demonstrate that the simultaneous occurrence of brittle and ductile deformation patterns observed in the field can be explained by self-localizing thermal runaway at differential stresses lower than those required for brittle failure. Our results suggest that by perturbing rock properties, weakening by hydration also plays a key role in shear zone formation and seismic failure; however, thermal runaway enables the rocks to fail in the absence of a free fluid phase.

The intense seismicity in subduction zones at depths greater than 50 km has puzzled geoscientists for decades because high ambient pressures should inhibit brittle failure at such depths. Two main failure mechanisms for intermediate-depth earthquakes have been hypothesized: (1) dehydration embrittlement and (2) shear instabilities. Metamorphic dehydration reactions have the potential to raise the pore fluid pressure and thereby lower the effective pressure to values that permit brittle failure^{4–6}. Elastic energy stored in a viscoelastic material may be spontaneously released at seismic strain rates by the formation of very high-temperature self-localizing shear instabilities^{1,3,7}, and the most unknown critical factor for this failure mode is the conditions under which an initial perturbation of the system either decays or self-amplifies, leading to extreme localization of deformation and shear heating. Both mechanisms are theoretically viable but it is difficult to discriminate between them.

Pseudotachylyte fault veins (quenched melts) provide evidence for paleo-earthquakes⁸, and they can be used to study the details of seismic failure. It has been suggested that pseudotachylytes associated with shallow earthquakes (10–15 km depth) are usually formed by brittle failure followed by frictional melting⁹, but at low background temperatures and high stresses ductile deformation

facilitated by thermal feedback and rock weakening due to dynamic recrystallization may also lead to seismic slip^{10,11}. High-pressure pseudotachylytes are found in exhumed deep continental rocks^{12–14} and in exhumed fragments of subducted oceanic slabs^{15–17}. These observations show that extreme shear heating may play an active role in earthquakes at high confining pressures. However, under these conditions it is questionable whether brittle failure precedes deformational melting. We present results of detailed studies of eclogite-facies pseudotachylytes and a theory for intermediate-depth earthquakes that is consistent with the geological evidence. We propose that self-localizing thermal runaway (SLTR) is the failure mechanism.

Whereas ref. 1 quantified the conditions under which viscoelastic materials fail by SLTR, we focus on the applicability of this theory to intermediate-depth earthquakes. In this setting, brittle deformation is prohibited by the high confining pressures. Nevertheless, the high shear stress will be relaxed, and parts of the initial elastic energy will be converted into heat, even without macroscopic deformation. Because of rock heterogeneity, preferential heating will occur in domains of lower effective viscosity, and this will amplify the initial effective viscosity variation. Mechanical energy dissipation due to ductile shearing will cause additional temperature increase and further localization of the initial spatial heterogeneity. This positive feedback eventually leads to SLTR relaxation of differential stresses by intensely localized shear and possibly coseismic deformation. This mechanism, based on ductile shear zone formation before the seismic rupture, requires no brittle failure.

The Precambrian Kråkenes gabbro, located within the Caledonian (410 ± 10 Myr) high- to ultrahigh-pressure metamorphic Western Gneiss Complex (WGC) in Norway, provides a spectacular example of intensely localized shear failure of rocks at high confining pressures¹³. The almost pristine gabbro is transected by a swarm of alternating shear zones and pseudotachylyte fault veins that share the same structural orientation and can be traced over several tens of metres¹³. The WGC formed the root zone of the Caledonides and experienced a regional southeast–northwest temperature–pressure gradient with temperatures T ranging from 600 to 850 °C and pressures P ranging from 1.6 to more than 3 GPa (ref. 18). The gabbro was deformed and metamorphosed ($T \approx 650$ – 700 °C; $P \approx 2$ GPa) during the Caledonian orogeny^{13,18}. Deformation and metamorphism are always associated with infiltration of external fluids and the fluids caused the infiltrated parts of the gabbro to become more reactive and thereby weaker relative to their dry precursors^{19–21}. However, some internal parts of the body in which fluid infiltration was inhibited show no overprint,

¹Physics of Geological Processes (PGP), University of Oslo, PO Box 1048, Blindern, N-0316, Oslo, Norway, ²The Future Ocean, IFM-GEOMAR, Wischhofstr. 1–3, 24148 Kiel, Germany. *Present address: Institut für Mineralogie, Universität Münster, Corrensstr. 24, 48149 Münster, Germany.

†e-mail: timm.john@uni-muenster.de.

and hence the protolith and evidence of the incipient local shear failure¹³ was preserved. This gabbro is also linked with subduction zone earthquakes, because (1) relatively dry gabbro constitutes most of the lower oceanic crust, (2) the kinetically delayed conversion of oceanic gabbro to eclogite during subduction is often associated with intermediate-depth seismicity and (3) the P - T conditions of the WGC are representative of intermediate-depth earthquakes in subducting slabs^{5,6,15,16,22–25}.

The shear zones have maximum widths of 5 cm, with cores of intensely deformed material surrounded by reaction haloes in which deformation is less obvious (Fig. 1a). Water-bearing minerals are concentrated in shear zones and their abundance decreases towards the deformation front. The metamorphic minerals form strongly deformed symplectites, with grain sizes that are approximately a thousand times smaller than those of the magmatic precursor minerals (Figs 1a and 2a). The symplectites surround only vaguely deformed magmatic clinopyroxene relicts (Fig. 2a). Even very limited subsequent reactivation of deformation would have erased the delicate symplectite textures, indicating that the shear zone was formed during a single event, and that the adjacent wall rocks did not experience polyphase deformation.

Pseudotachylyte fault veins are less than 1 cm thick with sharp contacts to the wall rocks, which are only locally fractured and injected by veins (Fig. 1b). Pseudotachylytes contain μ m- to mm-scale amoeboid and dendrite-like textures of garnet and plagioclase intergrown with eclogite-facies minerals including orthopyroxene, omphacite and amphibole (Fig. 2b), which evince rapid disequilibrium crystallization under high-pressure conditions. These quench textures are formed by rapid solid-state ripening of a microcrystalline matrix¹³. Like the shear zones, the pseudotachylytes record single, rapid events, as the delicate internal textures otherwise would have been erased by even minor reactivated deformation and/or recrystallization. Neither shear zones nor coexisting pseudotachylytes show evidence of a multiphase history, and it is therefore likely that they are manifestations of the same deformation event.

The key observations are that (1) cofacial, eclogite-facies shear zones and pseudotachylytes coexist, (2) both have higher degrees of hydration, caused by infiltration of external fluids, and up to three-orders-of-magnitude-smaller grain sizes than the almost dry wall rock, and (3) both types formed in a single, continuous and fast event. A quantitative model of intermediate-depth seismicity should account for the geological observations outlined above. In particular, the model should explain fault veins with quenched cores and undeformed margins coexisting with un-molten shear zones ($\gamma \approx 3$; 300% shear strain) and causal links between the two. The model of ref. 1 was modified to account for latent heat of melting and the drop in effective viscosity of molten material. The presence of hydrous mineral assemblages in the shear zone and pseudotachylyte led us to consider local perturbations of material properties. The intensity of the perturbation is given by δ , the ratio of initial effective viscosities of the background and hydrated rocks. In our numerical simulations, we use $\delta \approx 100$ estimated from the reduced activation energy for creep due to hydrous minerals and a reduced viscosity coefficient due to grain-size reduction associated with initial hydration reactions (see Supplementary Information, Table S1).

Two numerical simulations were designed to analyse how gabbro reacts to imposed stress and to demonstrate that a one-dimensional model of thermal runaway is consistent with the field observations. Both simulations used an ambient temperature of 680 °C, an initial differential stress of 1.5 GPa and the rheology of diabase²⁶. Diabase was chosen because it is a fine-grained equivalent to a gabbro and a grain-size-independent flow law (dislocation creep) was used. The models share the same geometry with a perturbed zone 600 times smaller than the model domain, in accordance with the field observations. The only difference between the models is in

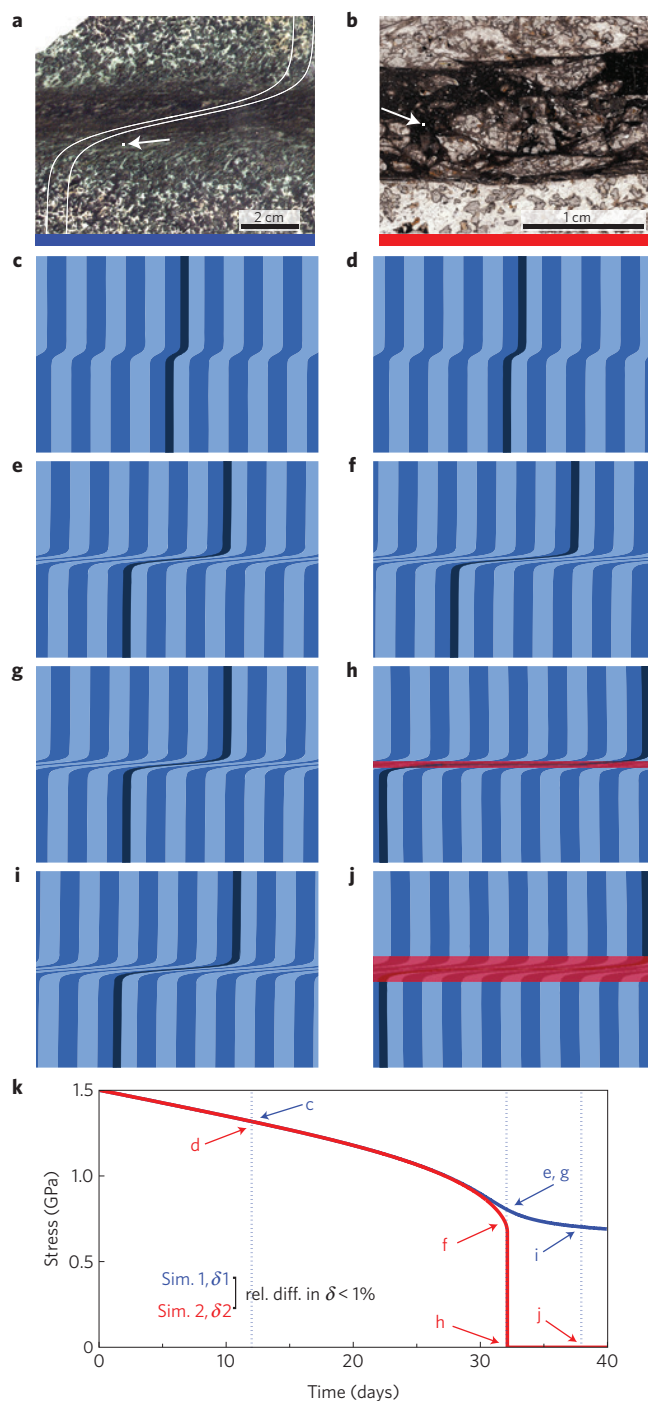


Figure 1 | Comparison of field observations with the numerical simulations. **a, b**, Photomicrographs of a typical shear zone (**a**) and a pseudotachylyte (**b**) from the Kråkenes gabbro. The shear zone shows no signs of melting, whereas the pseudotachylyte has a molten core and limited deformation at the margins. **c–j**, The results of two numerical simulations that reproduce the observed structures. The left-hand column (**c, e, g, i**) illustrates a shear-zone-forming simulation (1) and the right-hand column (**d, f, h, j**) a pseudotachylyte-forming simulation (2). Both columns show the evolution of passive markers together with regions of complete melting (red) for model times shown in the lower plot (**k**). **k**, The time dependence of the stress. The predicted unloading of Simulation 1 (**g**) and the thermal relaxation in Simulation 2 (**j**) are fully consistent with the strain marker patterns recorded in the field. The white curves in **a** are initially vertical lines with the deformation field from **g**. The images in Fig. 2 show the microstructure at the white arrows in **a, b**.

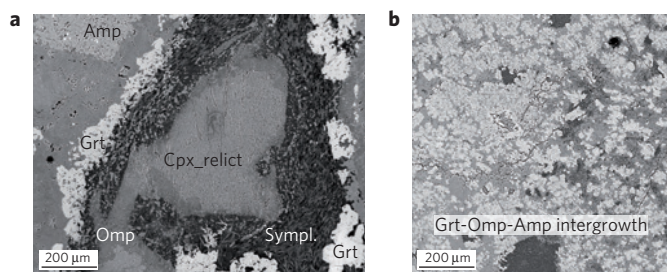


Figure 2 | Microstructures of a hydrous shear zone and a hydrous pseudotachylyte. **a**, Hydrous shear zone; **b**, hydrous pseudotachylyte. The delicate fine-grained eclogite-facies textures visible in both images indicate that no reactivation or recrystallization occurred after the primary deformation event. Even minor secondary deformation, reactivation and/or recrystallization would have erased the observed textures (Amp—amphibole; Omp—omphacite; Grt—garnet; Symp.—symplectite consisting mainly of albite + clinozoisite + amphibole; Cpx_relict—magmatic clinopyroxene relict).

the slightly lower (<1%) initial effective viscosity of the perturbed zone in simulation (2). Figure 1 shows the simulated deformation pattern at four different times. During the first phase (up to the time corresponding to Fig. 1e,f) the two simulations develop similarly and create similar shear zones.

Although the difference between the initial conditions is minor (<1% in δ), the final results are dramatically different, and this sharp transition is consistent with the theory of ref. 1. Although the deformation in simulation (1) becomes localized and the stress drop during the evolution from the time corresponding to Fig. 1e to that corresponding to Fig. 1g is significant (200–300 MPa), the temperatures never exceed 780 °C and no melts are formed. The shear zone predicted by the model is strikingly similar to shear zones in the field (see Fig. 1a,g). In contrast, the transition from the time corresponding to Fig. 1f to the time corresponding to Fig. 1h in simulation (2) results in catastrophic thermal runaway with localization ($\gamma > 10^3$ in the central part of the zone, which is less than 1 mm wide), a stress drop of ~750 MPa in milliseconds, extensive shear heating that melts the deformation zone (Fig. 1h), and no subsequent deformation. The thermal field in simulation (2) continues to evolve after the initial melting (Fig. 1h–j), and this is consistent with the observed microstructures that indicate stress-free crystallization (Fig. 2b). The final product is a quenched fault-vein with undeformed margins, analogous to field observations (Fig. 1j,b). The second phase of simulation (2) (Fig. 1h) unloads the system owing to the rupture (earthquake) and the stress drop would terminate further evolution of the shear zone in simulation (1). This illustrates that the two modes of deformation may coexist with the same structural orientation and may occur during a single, non-reactivated event.

The numerical simulations provide strong support for the idea that SLTR is a viable mechanism for intermediate-depth earthquakes, under conditions corresponding to those of the metamorphic assemblages in the studied gabbro. An initial stress of 1.5 GPa is chosen in our simulations. We do not address the stress build-up process, but find that the initial conditions used are consistent with laboratory deformation experiments^{27–29} so that in the context of strain localization and potential local stress amplification (for example asperity stresses) use of a 1.5 GPa initial stress for modelling is reasonable. More elaborate simulations that include continuous stress loading and weakening due to fluid infiltration or low-temperature plasticity at high confining pressures²⁹ could significantly lower the stress required to initiate SLTR (see Supplementary Information, Figs S3,S4). The calculated stress drops of about 750 MPa are similar to the conservative

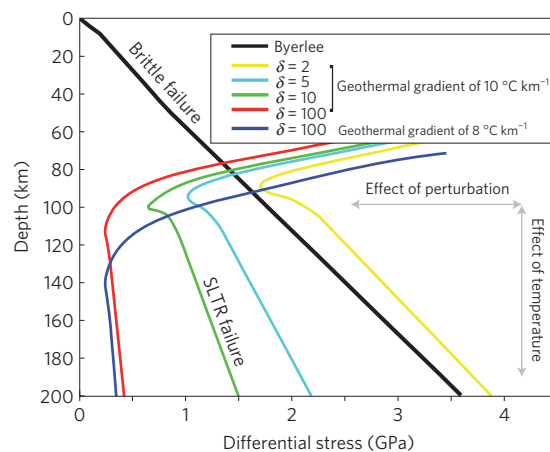


Figure 3 | Comparison of failure envelopes of SLTR (coloured lines) and Byerlee brittle failure (black line). The different colours indicate different SLTR parameters. For a wide parameter range, SLTR occurs at lower differential stresses than brittle failure at depths greater than 70 km. Lower geothermal gradients result in a deeper crossover point whereas bigger perturbations (induced by fluid infiltration) result in lower yield stresses. For typical subduction zone geothermal gradients, SLTR is the preferred failure mechanism because it occurs at lower differential stresses. Byerlee brittle failure stress was calculated for a compressional regime assuming zero fluid pressure.

estimates in ref. 17, which showed that paleo-earthquakes in a subduction setting have stress drops of at least 580 MPa. It is also in agreement with seismological evidence that points to stress drops up to 250 MPa (see ref. 30).

Figure 3 shows that the critical stress required to initiate SLTR depends on the average geothermal gradient and initial viscosity perturbation. Comparison of critical stresses with the Byerlee-law brittle yield stress shows that the crossover between failure modes occurs at 60–80 km, comparable to the characteristic pressures of blueschist-to-eclogite-facies metamorphic terrains. At hotter geotherms, the crossover usually occurs at shallower depths, but requires more intense perturbations (see Supplementary Information, Fig. S5). Our findings imply that at greater depths failure by SLTR is more likely than brittle failure, and that SLTR is a viable mechanism for intermediate-depth earthquakes in subducting slabs and continental root zones. SLTR, tested by the combined petrological and numerical study, is an alternative to dehydration embrittlement. Fluids play a major role in both mechanisms, but, in contrast to dehydration embrittlement, the fluid weakening in SLTR is accomplished without a free fluid phase because it is based mainly on an existing perturbation.

Received 25 June 2008; accepted 19 December 2008; published online 25 January 2009

References

- Braeck, S. & Podladchikov, Y. Y. Spontaneous thermal runaway as an ultimate failure mechanism of materials. *Phys. Rev. Lett.* **98**, 095504 (2007).
- Wright, T. W. *Cambridge Monographs on Mechanics* 241 (Cambridge Univ. Press, 2002).
- Kelemen, P. & Hirth, G. A periodic shear-heating mechanism for intermediate-depth earthquake in the mantle. *Nature* **446**, 787–790 (2007).
- Green, H. W. & Houston, H. The mechanics of deep earthquakes. *Annu. Rev. Earth Planet. Sci.* **23**, 169–213 (1995).
- Kirby, S. H., Engdahl, E. R. & Denlinger, R. P. in *Subduction Top to Bottom* (eds Bebout, G. E., Scholl, D. W., Kirby, S. H. & Platt, J. P.) 195–214 (Geophysical Monograph 96, American Geophysical Union, 1996).
- Hacker, B. R., Peacock, S. M., Abers, G. A. & Holloway, S. D. Subduction factory 2. Are intermediate-depth earthquakes in subducting slabs linked to metamorphic dehydration reactions? *J. Geophys. Res.* **108**, 1–16 (2003).

7. Ogawa, M. Shear instability in a viscoelastic material as the cause of deep focus earthquakes. *J. Geophys. Res.* **92**, 13801–13810 (1987).
8. Sibson, R. H. & Troy, V. G. The habitat of fault-generated pseudotachylite: Presence versus absence of friction-melts. *Geophys. Monogr. Ser.* **170**, 153–166 (2006).
9. Di Toro, G., Hirose, T., Nielsen, S., Pennacchioni, G. & Shimamoto, T. Natural and experimental evidence of melt lubrication of faults during earthquakes. *Science* **311**, 647–649 (2006).
10. Hobbs, B. E., Ord, A. & Teyssier, C. Earthquakes in the ductile regime? *Pure Appl. Geophys.* **124**, 309–336 (1986).
11. Obata, M. & Karato, S.-I. Ultramafic pseudotachylite from the Balmuccia peridotite, Ivrea-Verbano zone, northern Italy. *Tectonophysics* **242**, 313–328 (1995).
12. Austrheim, H. & Boundy, T. M. Pseudotachylites generated during seismic faulting and eclogitization of the deep crust. *Science* **265**, 82–83 (1994).
13. Lund, M. G. & Austrheim, H. High-pressure metamorphism and deep-crustal seismicity: Evidence from contemporaneous formation of pseudotachylites and eclogite-facies coronas. *Tectonophysics* **372**, 59–83 (2003).
14. Steltenpohl, M. G., Kassos, G. & Andresen, A. Retrograded eclogite-facies pseudotachylites as deep-crustal paleoseismic faults within continental basement of Lofoten, north Norway. *Geosphere* **2**, 61–72 (2006).
15. Austrheim, H. & Andersen, T. B. Pseudotachylites from Corsica: Fossil earthquakes from a subduction complex. *Terra Nova* **16**, 193–197 (2004).
16. John, T. & Schenk, V. Interrelations between intermediate-depth earthquakes and fluid flow within subducting oceanic plates: Constraints from eclogite-facies pseudotachylites. *Geology* **34**, 557–560 (2006).
17. Andersen, T. B., Mair, K., Austrheim, H., Podladchikov, Y. Y. & Vrijmoed, J. C. Stress-release in exhumed intermediate-deep earthquakes determined from ultramafic pseudotachylite. *Geology* **36**, 995–998 (2008).
18. Labrousse, L. *et al.* Pressure–temperature–time–deformation history of the exhumation of ultra-high-pressure rocks in the Western Gneiss Region, Norway. *Geol. Soc. Am. Spec. Paper* **380**, 155–183 (2004).
19. Austrheim, H. Eclogitization of lower crustal granulites by fluid migration through shear zones. *Earth Planet. Sci. Lett.* **81**, 221–232 (1987).
20. Karato, S.-I. & Jung, H. Effects of pressure on high-temperature dislocation creep in olivine. *Phil. Mag.* **83**, 401–414 (2003).
21. Kohlstedt, D. L. in *Water in Nominally Anhydrous Minerals* (eds Keppler, H. & Smyth, J. R.) 377–396 (Reviews in Mineralogy and Geochemistry, Vol. 62, 2006).
22. Hacker, B. R. in *Subduction Top to Bottom* (eds Bebout, G. E., Scholl, D. W., Kirby, S. H. & Platt, J. P.) 337–346 (Geophysical Monograph 96, American Geophysical Union, 1996).
23. Yuan, X. *et al.* Subduction and collision processes in the central Andes constrained by converted seismic phases. *Nature* **408**, 958–961 (2000).
24. Wayte, G. J., Worden, R. H., Rubie, D. C. & Droop, G. T. R. A TEM study of disequilibrium plagioclase breakdown at high pressure; the role of infiltrating fluid. *Contrib. Mineral. Petrol.* **101**, 426–437 (1989).
25. Rondenay, S., Abers, G. A. & van Keken, P. E. Seismic imaging of subduction zone metamorphism. *Geology* **36**, 275–278 (2008).
26. Mackwell, S. J., Zimmerman, M. E. & Kohlstedt, D. L. High-temperature deformation of dry diabase with application to tectonics on Venus. *J. Geophys. Res.* **103**, 975–984 (1998).
27. Li, L., Weidner, D., Raterron, P., Chen, J. & Vaughan, M. Stress measurements of deforming olivine at high pressure. *Phys. Earth Planet. Inter.* **143**, 357–367 (2004).
28. Boettcher, M. S., Hirth, G. & Evans, B. Olivine friction at the base of oceanic seismogenic zones. *J. Geophys. Res.* **112**, B01205 (2007).
29. Renshaw, C. E. & Schulson, E. M. Limits on rock strength under high confinement. *Earth Planet. Sci. Lett.* **258**, 307–314 (2007).
30. Kanamori, H. Mechanics of earthquakes. *Annu. Rev. Earth Planet. Sci.* **22**, 207–237 (1994).

Acknowledgements

We acknowledge discussions at PGP, particularly with S. Braeck, and proof reading by P. Meakin, G. Hirth and C. Marone provided constructive and helpful reviews. This study was supported by a Center of Excellence grant to PGP from the Norwegian Research Council.

Author contributions

All authors participated in collecting the data, interpretation of results and developing the model. T.J., T.B.A. and H.A. focused on the fieldwork, sampling and petrology, and T.J., S.M., L.H.R. and Y.Y.P. focused on the numerical simulations.

Additional information

Supplementary Information accompanies this paper on www.nature.com/naturegeoscience. Reprints and permissions information is available online at <http://npg.nature.com/reprintsandpermissions>. Correspondence and requests for materials should be addressed to T.J.